THE JOURNAL OF PHYSICAL CHEMISTRY B

Article

pubs.acs.org/JPCB

The Role of Different Structural Motifs in the Ultrafast Dynamics of Second Generation Protein Stains

Soumit Chatterjee,[†] Peter Karuso,*[,†] Agathe Boulangé,[§] Philippe A. Peixoto,[§] Xavier Franck,[§] and Anindya Datta*[,‡]

[†]Department of Chemistry and Biomolecular Sciences Macquarie University, Sydney, NSW 2109, Australia

[‡]Department of Chemistry Indian Institute of Technology Bombay, Powai, Mumbai 400076, India

[§]Normandie Univ, COBRA, UMR 6014 et FR 3038; CNRS; Univ Rouen; INSA Rouen, 1 rue Tesnières, 76821 Mont-Saint-Aignan Cedex, France

Supporting Information

ABSTRACT: Engineering the properties of fluorescent probes through modifications of the fluorophore structure has become a subject of interest in recent times. By doing this, the photophysical and photochemical properties of the modified fluorophore can be understood and this can guide the design and synthesis of better fluorophores for use in biotechnology. In this work, the electronic spectra and fluorescence decay kinetics of four analogues of the fluorescent natural product epicocconone were investigated. Epicocconone is unique in that the native state is weakly green fluorescent, whereas the enamine formed reversibly with proteins is highly emissive in the red. It was found that the ultrafast dynamics of the analogues depends profoundly on the H-bonding effect of solvents and solvent viscosity though solvent polarity also plays a role. Comparing the steady state and time-resolved data, the weak fluorescence of epicocconone in its native state is most likely due to the photoisomerization of the hydrocarbon side chain, while the keto enol moiety also has a role to play in determining the fluorescence quantum yield. This understanding is expected to aid the design of better protein stains from the same family.

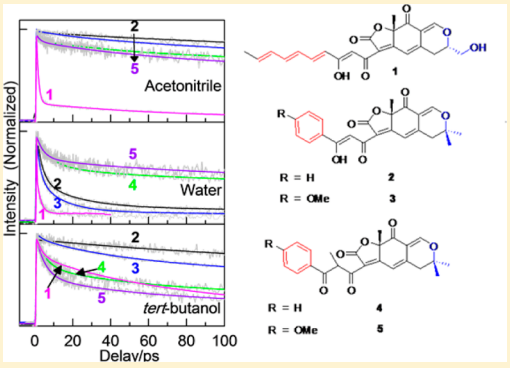

INTRODUCTION

Epicocconone (**1**, Scheme 1) is a fluorescent, cell permeable natural product isolated from the fungus *Epicoccum nigrum*.[1] Its enamine (**6**) is characterized by a high molar absorptivity (~10^4) at wavelengths provided by common lasers (488, 532 nm), strong fluorescence under specific conditions, a Stokes shift of ~100 nm, and a low cytotoxicity coupled with cell permeability.[2] These properties make it a potentially good fluorescent probe for biotechnological applications such as cell tracking and two-color staining, when multiplexed with other fluorescent probes which have similar absorbancies but different regions of emission. The conjugated β-diketone moiety in epicocconone is reminiscent of a similar structure in curcumin, a medicinal pigment from turmeric (*Cucuma longa* L).[3,4] The steady state behavior of both was found to be similar. The absorption maximum of curcumin is ~408−430 nm in most organic solvents, while the emission maximum is very sensitive to the solvent medium (460−560 nm). The fluorescence quantum yield of curcumin is low, and reduced significantly, in the presence of water, similar to epicocconone. The fluorescence lifetime is short (<1 ns) and the fluorescence decays are multiexponential, with contributions from ultrafast components of 10 and 70 ps. It was reported that solvation and excited state intramolecular proton transfer (ESIPT) are the main non-radiative pathways and the reasons for the low quantum yield of curcumin.[5,6] The structural similarity between the two fluorophores makes it tempting to rationalize the excited state dynamics responsible for the low fluorescence quantum yield of epicocconone on the basis of analogy with the photophysics of curcumin. Notably, epicocconone also is only weakly fluorescent at 530 nm in aqueous solutions but becomes strongly fluorescent with an emission maximum at 610 nm upon addition of proteins. This makes it an attractive fluorescent sensor for proteins, especially as it allows for the detection of proteins in gel electrophoresis down to <100 pg/band.[7,8] The enhancement of fluorescence of epicocconone in the presence of proteins has been shown to be due to reversible enamine formation with lysine residues.[9] This unique mechanism makes epicocconone the first reversible-covalent latent fluorophore to be discovered and has been used to develop novel enzyme assays based on fluorescence[10] and fluorescence anisotropy.[11] It has also been established that epicocconone is incorporated non-covalently into micelles and cyclodextrins and results in an increase in its green emission at

Received: September 17, 2013
Revised: October 22, 2013
Published: October 29, 2013

Scheme 1. Reaction of Epicocconone (1) and Analogues 2−5 with Butylamine (Magenta)[a]

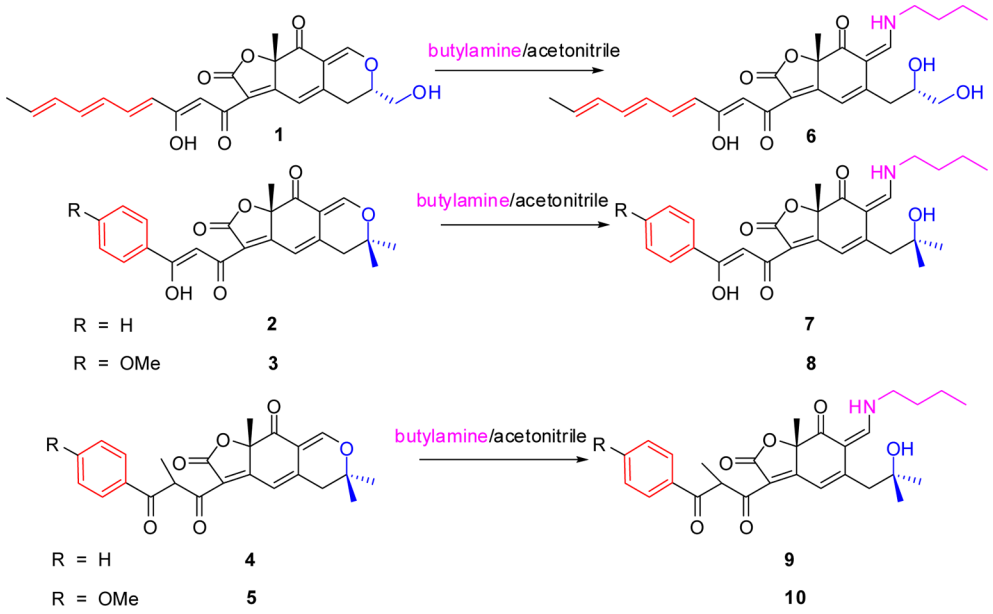

[a]The analogues **2** and **3** substitute the heptatriene side chain of epicocconone with an isoelectronic phenyl ring (red), the ethanol side chain (blue) is replaced with a *gem*-dimethyl, and the analogues **4** and **5** respectively substitute the keto-enol of **2** and **3** with a *β*-diketo group.

530 nm.[12,13] It has been proposed that photoisomerization, unlike solvation and excited state intramolecular proton transfer (ESIPT), which may be the primary non-radiative deactivation channel for this fluorophore, is suppressed in heterogeneous media, leading to the observed increases in quantum yield.[12] Using epicocconone butylamine adduct as a model of the protein adduct and assuming it underwent similar excited state dynamics, we proposed that the non-radiative process was due to either photoisomerization or excited state tautomerization which can be altered by solvent viscosity, solvent polarity, or H-bonding effects. To differentiate these alternative mechanisms and to understand the excited state dynamics of epicocconone, we synthesized epicocconone analogues that replaced the heptatriene tail with the homologous but unisomerizable phenyl (**2**) or anisyl (**3**) groups. The anisyl group additionally was designed to investigate the effect of resonance on the keto−enol. The keto−enol moiety was further substituted with a methyl, forcing a *β*-diketone in compounds **4** and **5**. These compounds all reacted with amines to form enamines in a similar fashion to **1** (Scheme 1).[9,14] The present study comprises the ultrafast dynamics of these epicocconone derivatives to understand the non-fluorescing behavior of epicocconone in solution.

In our earlier study, it was shown that both **1** and its butylamine adduct (**6**) undergo similar excited state processes. The predominant ultrafast component of 1 ps remained unchanged upon formation of the enamine. A slower component of 70 ps led to a population buildup of the actual emissive state. Rapid internal conversion (IC) provided a facile non-radiative channel of depopulation of this state, causing the fluorescence quantum yield of **1** to be rather small. The 1 ps component was tentatively assigned to photoisomerization of the heptatriene chain present in epicocconone, but excited state tautomerism could not be ruled out. Notably, the 1 ps component remained unchanged upon enamine formation of **1**. The 70 ps component, on the other hand, contributed to a greater extent in the enamine and was assigned to the flexing motion of the heteronuclear ring system, leading to the conformationally relaxed emissive state.[14]

MATERIALS AND METHODS

The synthesis of **2−5** is described elsewhere.[15] A solution of each compound in DMSO (1 mg/mL) was used as the stock solution for each experiment. Spectroscopy grade acetonitrile (Spectrochem, Mumbai, India) was distilled over CaH_2 and the distillate passed over activated neutral alumina prior to each experiment. Butylamine (Qualigens, Mumbai, India) and *tert*-butanol (spectroscopy grade, Spectrochem, Mumbai, India) were used as received. The absorption and fluorescence spectra have been recorded on a JASCO V 530 spectrophotometer and a Varian Cary Eclipse spectrofluorimeter, respectively. The emission spectra were recorded exciting at 410/400 nm with 5 nm of excitation and emission slit width and at 500 nm excitation for the butylamine adducts. The absorbancies of the solutions were kept below 0.1 to prevent inner filter effects for steady state measurements and for picosecond−nanosecond time-resolved experiments. The absorbancies of the solutions were kept at ∼1.0 for the upconversion experiments. The absorption and emission spectra were recorded before and after the femtosecond fluorescence decays in order to verify that the samples do not photodegrade. Fluorescence quantum yields of **1−5** (ϕ_f) were calculated after correction for changes in absorbance using Lucifer Yellow CH (ϕ_f = 0.21) as the reference.[16] Fluorescence quantum yields of **6−10** (ϕ_f) were calculated after correction for changes in absorbance using rhodamine 6G (ϕ_f = 0.94) as the reference.[17] Time-resolved fluorescence data were obtained using a picosecond pulsed diode laser based time-correlated single photon counting (TCSPC) instrument (IBH, United Kingdom) set at the magic angle with λ_{ex} = 406 nm. The full width at half-maximum (fwhm) of the instrumental response at this wavelength was found to be 250 ps with a resolution of 7 ps/channel. The decay traces, thus obtained, were fitted to multiexponential decays using IBH DAS 6.2 data analysis software. The output of

dx.doi.org/10.1021/jp4092927 | J. Phys. Chem. B 2013, 117, 14951−14959

a femtosecond pulsed oscillator from a mode-locked Ti:sapphire laser (Tsunami, Spectra Physics, USA) pumped by a 5 W DPSS laser (Millennia, Spectra Physics), centered at 800 nm and with a repetition rate of 80 MHz, was used as the gate pulse for the femtosecond fluorescence upconversion experiments. The second harmonic (400 nm) of this pulse was used as the source of excitation for the sample placed in a rotating cell. The power of the second harmonic light is restricted to 5 mW at the sample in order to minimize photobleaching. The fluorescence from the sample is upconverted in a nonlinear crystal (0.5 mm BBO, $\theta = 38°$, $\phi = 90°$) by mixing with the gate pulse, which consists of a portion of the fundamental beam. The upconverted light is dispersed in a monochromator and detected using photon counting electronics. A cross-correlation function obtained using the Raman scattering from ethanol has a fwhm of 300 fs. The femtosecond fluorescence decays have been fitted using a Gaussian function of the same fwhm as the excitation pulse. The fluorescence decays were recorded at the magic angle polarization with respect to the excitation pulse on an FOG 100 fluorescence optically gated upconversion spectrometer (CDP Systems Corp., Russia). The resolution was in appropriate multiples of the minimum step size of the instrument, i.e., 0.78 fs/step. The decays were analyzed by iterative reconvolution using a homemade program.[18] The lifetime found from the TCSPC was fixed to the longest component while fitting the fluorescence decay.

Computational results were generated using Turbomole (COSMOlogic).[19] Exhaustive conformational searches for the native and enamine adducts were performed with DFT-D3[20] calculations with the B88/P86[21] exchange-correlation functional using the TZVPP basis set[22] and a continuum solvent model for acetonitrile (COSMO).[23] Vertical excitations were calculated using time dependent density functional theory (TD-DFT), taking into account the 25 lowest excited states. The level of theory required to predict the actual UV spectra generally corresponded to the PBE0/TZVP level of theory.[24] Ground states were confirmed through frequency analyses.

RESULTS AND DISCUSSION

Epicocconone (**1**) and its butylamine adduct (**6**) showed absorption maxima at 435 and 520 nm, respectively, while their emission maxima appeared at 535 and 615 nm, respectively.[9,14]

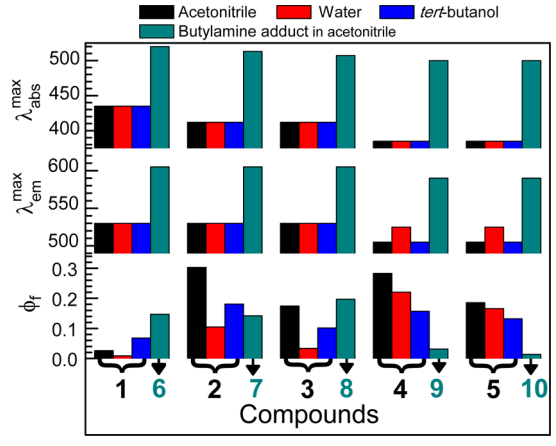

Figure 1. Summary of the spectral parameters of the fluorophores studied (**1**–**5**), in three solvents. The data for their butylamine adducts (**6**–**10**) in acetonitrile show the changes in spectral parameters upon enamine formation.

In the present study, we found the absorption maxima of compounds **2** and **3** (Scheme 1) to occur at 412–413 nm, while those of their butylamine adducts (**7** and **8**) were red-shifted to 513 and 507 nm, respectively (Figures 1, S1a and S1b, Supporting Information). The emission maxima were found at 530 nm for **2** and **3** and at 605 nm for **7** and **8** (Figures 1, S1a and S1b, Supporting Information). Thus, the trends in the spectral shifts upon enamine formation were quite similar to that seen for **1**. These data suggest that the aromatic ring is not involved in the lowest $\pi \rightarrow \pi^*$ transition, as the absorption and emission spectra of an anisole derivative would be expected to have a red shift of ∼20 nm compared to that of the benzene analogue due to the extra conjugation.[25−27] Hence, **2** and **3** were found to be excellent models to study the effect of the heptatriene chain of **1**, as no additional photophysics seemed to complicate the situation and the keto−enol moiety, present in **1**, was conserved in **2** and **3**. In the three solvents studied, the fluorescence quantum yields of **2** and **3** were always much larger than that of **1** (Figure 1, Table 1). This may be ascribed to the absence of the non-radiative decay channel provided by photoisomerization in the heptatriene chain in **2** and **3**. However, the quantum yield of **3** was lower than that of **2** in each of the three solvents, suggesting an additional non-radiative process in **3** associated with the methoxy group. This non-radiative process could be an ICT from the *p*-methoxyphenyl group. Thus, the heptatriene group was found to be a major contributor to the non-radiative process in **1**, leading to its very low quantum yield, especially in water. This feature is very useful when formation of the enamine is the species of interest.

Compounds **4** and **5** differed from **2** and **3** in that there was an extra methyl group between the two keto groups. The effect of this is to make keto−enol tautomerism impossible due to steric requirements of the methyl. This was evident experimentally from the NMR spectra of **4** and **5** (Supporting Information), which show a quartet, integrating for one proton at δ 5.5. In contrast, this proton appears at δ 7.1 as a singlet in **2** and **3** (cf. 6.8 ppm for **1**[1]). Similarly, in the ^{13}C NMR spectrum of **2** and **3** (Supporting Information), the carbon between the two carbonyls resonates at 97 ppm (cf. 101 ppm for **1**[1]), while for **4** and **5** this carbon resonates at ∼52.5 ppm. These data indicated that substituting C2′ with a methyl effectively inhibits keto−enol tautomerism in the ground state and these compounds could be used to look at the role of keto−enol tautomerism in the fluorescent properties of epicocconone. Computational results indicated compound **4** is 2.7 kcal/mol higher in energy in the keto−enol form (DFT//PBE0/TZVPP) than in the diketo form and that in the ground state the two keto groups are orthogonal in **4** and **5** in agreement with previous results.[24] Compounds **4** and **5** consequently show blue-shifted electronic absorption spectra, with maxima at ∼385 nm, compared to the maximum at ∼412 nm for **2** and **3**. The quantum yield of **4** is comparable with that of **2** in acetonitrile and *tert*-butanol but in water is 2 times higher (Figure 1, Table 1). Thus, the keto−enol group did not appear to play a major role in the non-radiative depopulation of the excited state of **1** and its analogues, in non-aqueous solvents. The quantum yield of **5** is lower than that of **4** in all three solvents—further evidence of an ICT in the *p*-methoxyphenyl derivatives. Hence, a unified picture of fluorophores **1**–**5** begins to emerge.

DFT calculations were used to investigate these four analogues more closely. A conformational search using

dx.doi.org/10.1021/jp4092927 | J. Phys. Chem. B 2013, 117, 14951−14959

Table 1. Molar Extinction Coefficients and Quantum Yields of Compounds 1−5 in Different Solvents

	ε (Lit.M^{-1} cm^{-1})					ϕ_f				
solvent	**1**[a]	**2**[c]	**3**[c]	**4**[e]	**5**[e]	**1**[b]	**2**[d]	**3**[d]	**4**[f]	**5**[f]
acetonitrile	13400	17600	11800	750	1400	0.026	0.303	0.175	0.283	0.186
water	11400	11100	1500	1160	1020	0.009	0.105	0.034	0.221[g]	0.166[g]
tert-butanol	15600	16200	3100	1270	840	0.068	0.181	0.102	0.157	0.132

[a]At λ = 435 nm. [b]At λ = 520 nm. [c]At λ = 410 nm. [d]At λ = 530 nm. [e]At λ = 385 nm. [f]At λ = 505 nm. [g]At λ = 525 nm.

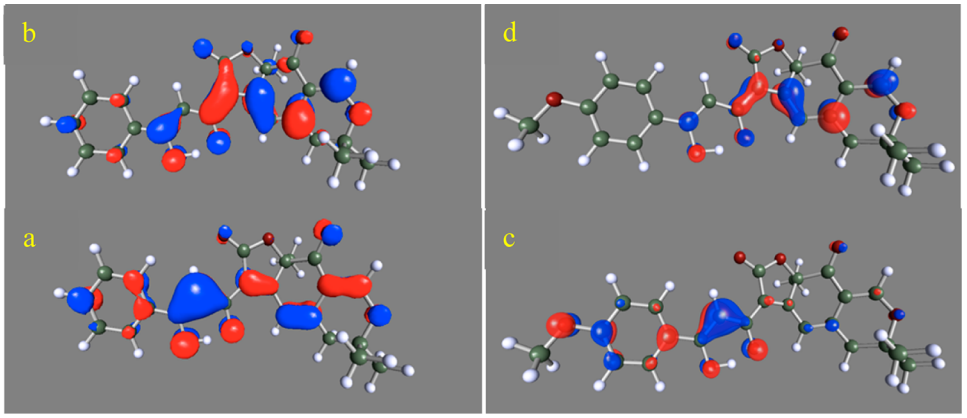

Figure 2. (a and c) HOMO (lower) and (b and d) LUMO (upper) calculated from geometry optimized **2** (left, a and b) and **3** (right, c and d) using the DFT-D3/BP86//TZVP basis set.

Table 2. Molar Extinction Coefficients and Quantum Yields of Compounds 6−10 in Acetonitrile

ε (Lit.M^{-1} cm^{-1})					ϕ_f				
6[a]	**7**[c]	**8**[e]	**9**[g]	**10**[g]	**6**[b]	**7**[d]	**8**[f]	**9**[h]	**10**[h]
13000	12630	9300	1645	2540	0.147	0.142	0.197	0.031	0.014

[a]At λ_{ex} = 520 nm. [b]At λ_{em} = 615 nm. [c]At λ_{ex} = 513 nm. [d]At λ_{em} = 605 nm. [e]At λ_{ex} = 507 nm. [f]At λ_{em} = 605 nm. [g]At λ_{ex} = 500 nm. [h]At λ_{em} = 590 nm.

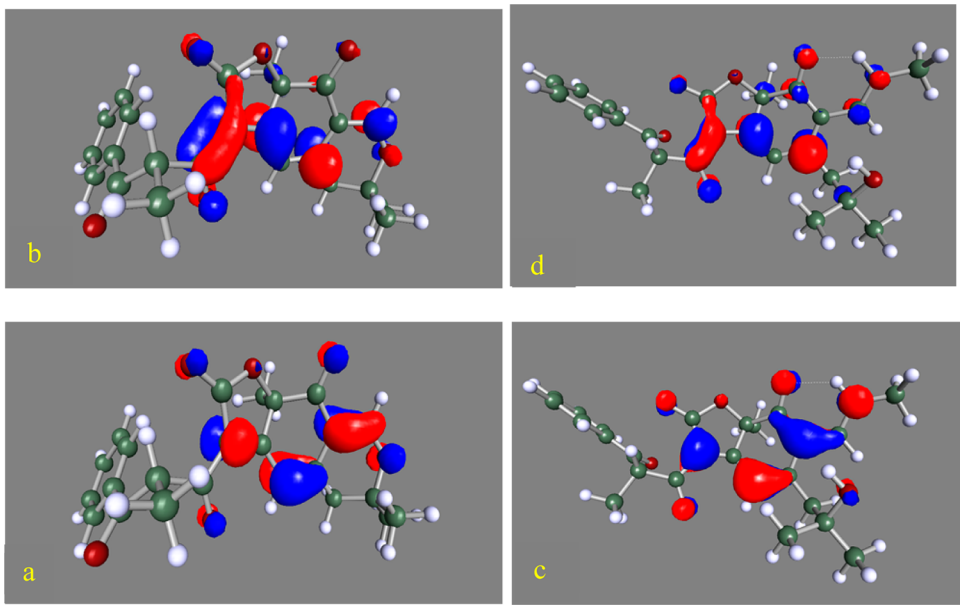

Figure 3. (a and c) HOMO (lower) and (b and d) LUMO (upper) of **4** (left, a and b) and **9** (right, c and d) showing that the two carbonyls are no longer coplanar and that the side chain (phenyl) is not involved in the photophysics.

DFT//B88-P86/S(V)P found 10 possible ground state conformers of **2**. The structures within 5 kcal/mol of the lowest energy were further geometry optimized (DFT-D3//B88-P86/TZVPP) using a continuum solvent model (COSMO) for water. For the β-diketone, enolization of the outer ketone was favored but only by about 1.4 kJ/mol (Figure S6, Supporting Information). The optimum length of the O−H was found to be 1.09 Å when on the outer oxygen and 1.12 Å when on the inner oxygen with an almost barrierless (0.03 kcal/mol) transition from the higher energy tautomer to the lower

dx.doi.org/10.1021/jp4092927 | J. Phys. Chem. B 2013, 117, 14951−14959

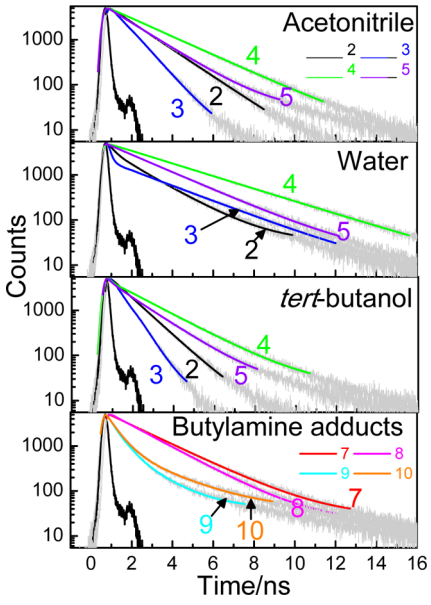

Figure 4. Nanosecond fluorescence decay traces of **2**−**5** in different solvents and the respective butylamine adducts, **7**−**10** in acetonitrile; λ_{ex} = 406 nm and λ_{em} = 530 nm for **2** and **3** in all solvents. λ_{em} = 505 nm for **4** and **5** in acetonitrile and *tert*-butanol, λ_{em} = 525 nm for **4** and **5** in water, λ_{em} = 605 nm for **7** and **8**, and λ_{em} = 590 nm for **9** and **10**.

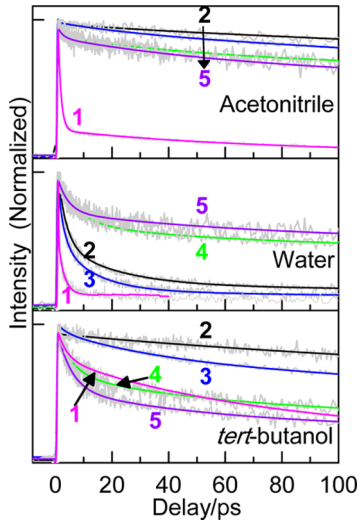

Figure 5. Femtosecond fluorescence transients of **1**−**5** in different solvents in 100 ps scale. λ_{ex} = 400 nm and λ_{em} = 530 nm for **2** and **3** in all solvents. λ_{em} = 505 nm for **4** and **5** in acetonitrile and *tert*-butanol and λ_{em} = 525 nm for **4** and **5** in water. The fitting parameters are provided in Tables S3−S6 (Supporting Information).

(Figure S6, Supporting Information). Other conformers and tautomers were of higher energy and not further considered. These results correlated well with those recently published except that we found that the second carbonyl is enolized for all the analogues.[28] The steady state UV spectra of **2** and **3** were calculated from the lowest energy structures (TD-DFT//pbe0/TZVP) and matched reasonably well with the actual spectra in acetonitrile (Figure S7, Supporting Information). We thus had confidence that the molecular orbitals would be well described at this level of theory. Plotting the HOMO and LUMO of **2** and **3** (Figure 2) revealed that **3** did in fact form an intramolecular ICT that was not as obvious in **2**. The

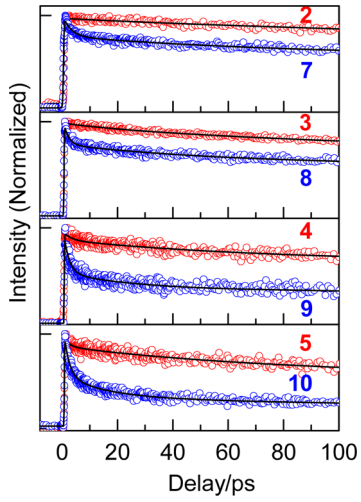

Figure 6. Femtosecond fluorescence transients of **2**−**5** (red ○) and **7**−**10** (blue ○) in acetonitrile in 100 ps scale. λ_{ex} = 400 nm and λ_{em} = 530 nm for **2** and **3**, λ_{em} = 530 nm for **4** and **5**, λ_{em} = 605 nm for **7** and **8**, and λ_{em} = 590 nm for **9** and **10**. The fitting parameters are provided in Tables S3−S6 (Supporting Information).

HOMO of **3** is associated with the anisyl-keto−enol, while the LUMO is associated more with the tricyclic nucleus common to **1**−**5**.

For complicated fluorophores like epicocconone, one needs to consider additional possibilities of excited state tautomerism, H-bonding with solvent, or changes in pK_a in the excited state. The pK_a's of **1**−**5** in the ground state (absorption at 406 nm) were all about the same (5.7 ± 0.1) but in the excited state increased for **1**−**3** but not **4** and **5** (Figures S2−S5, Table S1, Supporting Information). This suggests that in the excited state for compounds **1**−**3** the enol proton is more tightly held in the excited state, leading to an increase in pK_a, and that there is no effect of the methoxy group on the pK_a, indicating that there is little, if any, inductive effect on the keto−enol moiety. This supports the steady-state UV−vis absorptions where no bathochromic shift is observed for **3** over **1** or **2** and the computational results. Hence, the possibility of tautomerism or change in pK_a of the keto−enol to alter the dynamics of epicocconone can be ruled out.

Because of the utility of epicocconone in biotechnological applications, which rely on its conversion to a highly emissive enamine, a more pertinent question is the difference in photophysics brought about by enamine formation of our analogues. Upon formation of the butylamine adduct **6**, the quantum yield increases 6.5 times in acetonitrile compared to **1** but **7** decreases 2-fold with respect to **2**, while **8** shows a similar quantum yield to **3** (Figure 1, Table 2). Large Stokes shifts were observed in all cases, in accordance with the postulated enamine formation.[9] Enamines **6**−**8** all have quite similar quantum yields, absorption spectra, and Stokes shifts suggesting that enamine formation trumps any effects of the side chain.

In compounds **4** and **5**, the HOMO and LUMO orbitals do not involve the side chain, which explains their almost identical steady state behavior. This trend is also seen in the enamines **9** and **10** (Figure 3).

8 has a larger quantum yield than **7**, despite having the *p*-methoxy group which appears to be responsible for a lower quantum yield of **3** than **2**. The reason for this apparent anomaly is not very clear at this point, but it is possible that a charge transfer from the nitrogen atom in the enamine moiety

dx.doi.org/10.1021/jp4092927 | J. Phys. Chem. B 2013, 117, 14951−14959

Table 3. Average Lifetimes, Quantum Yields, and Radiative and Non-Radiative Rate Constants for Compounds 2−5

	2				3				4				5			
solvent	$\langle\tau\rangle$ (ns)	ϕ_f	$k_R \times 10^9$ s^{-1}	$k_{NR} \times 10^9$ s^{-1}	$\langle\tau\rangle$ (ns)	ϕ_f	$k_R \times 10^9$ s^{-1}	$k_{NR} \times 10^9$ s^{-1}	$\langle\tau\rangle$ (ns)	ϕ_f	$k_R \times 10^9$ s^{-1}	$k_{NR} \times 10^9$ s^{-1}	$\langle\tau\rangle$ (ns)	ϕ_f	$k_R \times 10^9$ s^{-1}	$k_{NR} \times 10^9$ s^{-1}
CH_3CN	0.86	0.30	0.35	0.81	0.68	0.18	0.26	1.21	1.14	0.28	0.25	0.63	0.84	0.19	0.23	0.96
water	0.11	0.11	1.00	8.09	0.04	0.03	0.75	24.25	0.96	0.22	0.23	0.81	0.84	0.17	0.20	1.00
tert-BuOH	0.82	0.18	0.22	1.00	0.39	0.10	0.26	2.30	0.42	0.16	0.38	2.00	0.25	0.13	0.52	3.48

Table 4. Average Lifetimes, Quantum Yields, and Radiative and Non-Radiative Rate Constants for Compounds 7−10 in Acetonitrile

	7				8				9				10			
solvent	$\langle\tau\rangle$ (ns)	ϕ_f	$k_R \times 10^9$ s^{-1}	$k_{NR} \times 10^9$ s^{-1}	$\langle\tau\rangle$ (ns)	ϕ_f	$k_R \times 10^9$ s^{-1}	$k_{NR} \times 10^9$ s^{-1}	$\langle\tau\rangle$ (ns)	ϕ_f	$k_R \times 10^9$ s^{-1}	$k_{NR} \times 10^9$ s^{-1}	$\langle\tau\rangle$ (ns)	ϕ_f	$k_R \times 10^9$ s^{-1}	$k_{NR} \times 10^9$ s^{-1}
CH_3CN	0.81	0.14	0.17	1.06	0.92	0.20	0.22	0.87	0.20	0.03	0.15	4.85	0.16	0.01	0.06	6.19

dx.doi.org/10.1021/jp4092927 | J. Phys. Chem. B 2013, 117, 14951−14959

is hindered by charge transfer in the opposite direction in the presence of the *p*-OMe group, somewhat like the hindrance of the more efficient flip-flop motion of the dimethylamino group in 3-aminoquinoline,[29] by an intramolecular charge transfer process. This argument gains some credence from the fact that this anomalous behavior was not observed while comparing **9** with **10**. Clearly, charge transfer from the anisyl group to the rest of the molecule is hindered in **10** because it is not actually conjugated with the fluorescent core and so the two charge transfer processes are not coupled in **10**, unlike in **8**. Another intriguing observation in this regard was the miniscule quantum yields of **9** and **10** (Figure 1, Table 2). This might also be explained in the light of a more efficient ICT from the enamine group in these adducts and a decrease in the efficiency of the non-radiative process due to an opposing ICT in **7** and **8**.

The fluorescence decays in the nanosecond time regime follow the same trend in the three solvents (Figure 4). The decays of **2** are slower than those of **3**, while the decays of **4** are slower than those of **5**. This observation was in line with the contention about a more efficient non-radiative deactivation by ICT in the presence of anisyl groups. Moreover, the decays of **4** were slower than those of **2** and the decays of **5** were slower than those of **3**, indicating that the keto−enol group did have a role to play in the excited state dynamics. However, the possibility of faster dynamics in the picosecond regime, analogous to that observed for **1**, needs to be considered before drawing an inference from the time-resolved data, as such ultrafast dynamics is capable of affecting the photophysics of these molecules rather drastically. Indeed, an ultrafast component of 2−3 ps was observed for **2** and **3** in water, with a contribution of 50%. This component was not obtained in acetonitrile or *tert*-butanol (Figure 5, Tables S6 and S7, Supporting Information). Thus, the picosecond dynamics of **2** and **3** was found to be slower than that in **1**. It may be recalled that, for **1**, a sub-picosecond ultrafast component was predominant in water as well as in acetonitrile and this component was assigned to the photoisomerization of the heptatriene chain.[13] Absence of the sub-picosecond component for **2** and **3**, which have the heptatriene replaced with an isoelectronic phenyl group, supports our assignment of this component to photoisomerization.[12,14] The 2−3 ps component observed for **2** and **3** can be assigned to intramolecular charge transfer (ICT), as its contribution was more prominent in water, indicating the involvement of a polar excited state. Faster decays in **3** can be rationalized in terms of more facile ICT, due to the presence of the anisyl group, as predicted by DFT calculations. Thus, it appears that, in the absence of photoisomerization, ICT plays a dominating role in the photophysics of epicocconone derivatives. Since the ICT in **2** was suppressed in the more viscous *tert*-butanol, it is likely to be associated with some bond twisting as well. A relatively slower component of 20−80 ps was found for **2** as well as **3** in all three solvents. This component may be assigned to the flexing of the tricyclic system to populate the emissive state, as was shown for **1**.[14] Compounds **4** and **5** had almost identical picosecond decay profiles in acetonitrile, with a 10% contribution of a 2 ps component. In water and *tert*-butanol, relatively slower components (4−7 ps) were observed (Figure 5, Tables S8 and S9, Supporting Information). Unlike in **2** and **3**, the slower components were ca. 50 ps in all three solvents. The slightly lower quantum yield of **4** (ϕ_f = 0.283, Table 1) than **2** (ϕ_f = 0.303, Table 1) in acetonitrile can be rationalized by the ultrafast component present in **4**. The difference in quantum yields of **3** and **5** can only be explained on the basis of their longer average lifetime. Radiative and non-radiative decay rates of these compounds in different solvents have been calculated in an attempt to generate a more quantitative understanding of the quantum yields.

So far, a comparison has been made between the temporal profiles of **2** and **3** and between those of **4** and **5** in acetonitrile, in an attempt to understand the role of ICT in these molecules. Upon a similar comparison for the other two solvents studied, it appears that qualitatively, the trends are similar. Decays for **3** are faster than **2**, while **5** has faster decays than **4** (Figures 4 and 5), suggesting that ICT plays an important role in the photophysics of **2**−**5**. The next question to address is the role of the keto−enol group in this ICT process. DFT calculations indicate that the two carbon−oxygen bonds are coplanar in **2** and **3** but not in **4** or **5**.[28] This may be rationalized in the light of the intramolecular hydrogen bond between the keto and enol groups in **2** and **3** and lack thereof between the two keto groups in **4** and **5**. It is possible that such coplanarity, or lack thereof, can favor (or hinder) ICT in these molecules. A comparison between the fluorescence decays of **2** and **4** and that between **3** with **5** is thus required. The nanosecond lifetimes of **4** were longer than those of **2** in all three solvents, while those of **5** were longer than those of **3** (Figure 4, Tables S2−S5, Supporting Information). Surprisingly, this trend was qualitatively opposite to that of fluorescence quantum yields (Figure 1, Table 1). For the picosecond components, this anomaly persists in acetonitrile and *tert*-butanol (Figure 5, Tables S6−S9, Supporting Information). In water, however, the fastest component in the keto−enol molecules (**2**, **3**) was of 2−3 ps, while that for the diketones (**4**, **5**) was 4−7 ps, with a decrease in their relative contribution. The slower picosecond component was ca. 15−20 ps in **2** and **3** but ca. 50 ps in **4** and **5**. This was in agreement with the order of quantum yields (**4** > **2** and **5** > **3**). Hence, we can infer that the diketo group does have a role to play in the photophysics of these compounds. The shorter picosecond components of the diketones compared to corresponding keto−enols indicate the occurrence of a more efficient non-radiative decay pathway in the diketones in acetonitrile and *tert*-butanol. This pathway is likely to be associated with the movement of the two carbonyl groups with respect to each other, which would be restricted in the intramolecularly hydrogen bonded keto−enol compounds. The anomalous observations in water are likely to arise from the competition to intramolecular hydrogen bond formation, offered by the solvent, which would tend to form intermolecular solute−solvent hydrogen bonds. The interplay of different factors that affect the non-radiative processes is best monitored by studying the non-radiative rates. This has been presented later in the manuscript, after a discussion of the temporal properties of the butylamine adducts.

The nanosecond lifetimes of butylamine adducts **8**, **9**, and **10** followed the same qualitative trends as quantum yields, when compared with their parent compounds **3**, **4**, and **5**, respectively. However, these trends are not quantitative. Upon going from **3** to **8**, the lifetime doubles, while the quantum yield increases by only 13%. Upon formation of the enamines of **4** and **5**, the lifetimes decrease to one-third and half of the lifetimes of the parent compounds, while the quantum yields decrease by an order of magnitude (Figure 1, Tables 1 and 2). This was an indication that, even in the enamines, picosecond dynamics plays an important role.

dx.doi.org/10.1021/jp4092927 | J. Phys. Chem. B 2013, 117, 14951−14959

Indeed, an ultrafast component of 2−3 ps, which was not observed in **2** and contributed little in **3**, was present to a significant extent (ca. 20%) for **7** and **8** in acetonitrile. The contribution of this component increased from ca. 10% in **4** and **5** to ca. 50% in **9** and **10** (Figure 6, Tables S8 and S9, Supporting Information). This component persisted in **9** and **10**, with an even greater contribution of ca. 50%. Thus, the contribution of the diketo moiety to the ultrafast non-radiative deactivation of the excited state appeared to be present in the enamines. On the other hand, the slower time constant was 20 ps in **7** and **8** (i.e., the enamines with the keto−enol moiety), while its value was 50 ps in **9** and **10** (i.e., the diketonic enamines). Thus, it appears that the conformational relaxation in enamines becomes faster in the diketo compounds. In addition, we found that the *p*-OMe had no role in the excited state dynamics of the butylamine adducts, as its presence did not lead to any change in the decay characteristics. Therefore, we can conclude that the nature of the *β*-diketone is the key factor guiding the excited state dynamics of the butylamine adducts while the side group remains inactive, which in turn supports and explains the dramatic increase in the quantum yield of **6**.[1,9,14]

The variation in fluorescence quantum yields between the four analogues in different solvents was investigated to understand the effects of hydrogen bonding on radiative and non-radiative decay rates (Table 3). Compounds **2** and **3** in acetonitrile showed similar radiative rate constants, while the non-radiative rate constant in **3** was ca. 1.5-fold higher than that of **2**, resulting in a higher quantum yield of **2** (Table 3). Similarly, in water and *tert*-butanol, a higher quantum yield of **2** than **3** can be ascribed to a lower non-radiative rate with respect to **3**. In water, the non-radiative rate constant was almost 3 times higher in **3** than that in **2**, thus accounting for the 3 times less quantum yield in **3** (Table 3). Similarly, a comparison between **4** and **5** in acetonitrile, water, and *tert*-butanol brings out the role of the non-radiative rates in the quantum yields. In **4** and **5**, non-radiative rates were found to be much slower in water, causing higher quantum yields in these compounds. We might therefore consider that the *p*-OMe causes an increase in the non-radiative rate for compounds while considering compounds of similar functional groups, i.e., for keto−enol bearing compounds like **2** and **3** or diketo compounds like **4** and **5**.

A comparison between **2** and **4**, in acetonitrile and *tert*-butanol, hints at the interplay of the radiative and non-radiative decay rates to elucidate the difference in their quantum yields. It can be found that **2**, having the keto−enol moiety, showed higher radiative and non-radiative decay rates simultaneously, but the radiative decay rate was found to be the key factor to explain the higher quantum yield of **2** over **4** (Table 3). This was not seen if **3** and **5** were compared in these solvents and the quantum yield was found to be a function of non-radiative decay rate, where **5**, having the diketo moiety, showed higher quantum yield than **3** (Table 3). In water, molecules having a keto−enol moiety had an almost 4-fold higher radiative rate constant with respect to the diketo counterpart, but it was the huge suppression of the non-radiative decay of the diketo compounds that led to a leap in their quantum yield (Table 3). We can conclude that the presence of a *p*-OMe group leads to an increase in the non-radiative rate in polar protic solvent for the keto−enol moiety bearing fluorophores. This could indicate the stabilization of a charge transfer state by the participation of hydrogen bonding with solvent molecules.

Comparing **7** and **8** (Table 4), a little lower quantum yield of **7** was found to be a result of the higher radiative rate constant of **7**. In the cases of **9** and **10** (Table 4), a similar trend was observed. Therefore, for the butylamine adducts, compounds having the *p*-OMe showed slightly higher radiative decay for keto−enol moieties but behaved oppositely for the diketo. In between **7** and **9**, it was found that the diketo group caused instability, resulting in an increase in non-radiative rate. This may be rationalized by the ICT from the enamine, which is less favorable in the case of diketo. The presence of *p*-OMe makes this process even unfavorable which is evident from the fact that, in between **8** and **10**, **10** not only showed a 7 times increase in the non-radiative rate, but also its radiative decay rate became faster by 2-fold, making it a very poor emitter in water.

CONCLUSION

In our earlier study, we postulated that photoisomerization or tautomerism of the *β*-diketone may be responsible for the non-fluorescing nature of epicocconone.[14] The present study, on four epicocconone analogues, establishes the involvement of photoisomerization of the heptatriene side chain, rather than the tautomerism of the *β*-diketone, as the major non-radiative process in epicocconone. This is manifested in the significantly higher fluorescence observed in the analogues that lack the conjugated chain. The corresponding butylamine adducts of the analogues showed a similar kind of reversible enamine formation with butylamine, as was evident from the red-shifted absorption and emission spectra. However, unlike epicocconone, they did not show the characteristic increase in quantum yield, suggesting that the heptatriene photoisomerization was not a significant relaxation pathway for the enamine of epicocconone. All the butylamine adducts (**6**−**8**) having a keto−enol moiety had comparable fluorescence intensities, indicating that intramolecular H-bonding helped stabilize the excited state. Compounds with a *β*-diketo group (**9**, **10**) had much lower quantum yields. This process can be affected by the intermolecular H-bonding with solvents, as found from the variation of the quantum yields of the analogues with different solvents. Other parameters like solvent polarity and viscosity can also play a crucial role in determining the fate of the excited state dynamics of these molecules. From our results, factors that increased quantum yield include photoisomerism in the heptatriene chain, flexing of the fused ring system, and a possible charge transfer involving the diketo group. This inference points the way to the design and synthesis of analogues with higher quantum yields. In order to obtain higher quantum yields, the heptatriene chain needs to be engineered so as to eliminate photoisomerization, while the keto enol moiety needs to be conserved in order to obtain a higher quantum yield for the butylamine adducts.

ASSOCIATED CONTENT

Supporting Information

Additional time-resolved decays, pK_a plots, computational data, and tables of decay parameters. This material is available free of charge via the Internet at http://pubs.acs.org.

AUTHOR INFORMATION

Corresponding Authors

*E-mail: peter.karuso@mq.edu.au. Phone: +612 9850 8290. Fax: +612 9850 8313.

*E-mail: anindya@chem.iitb.ac.in. Phone: +91 22 2576 7149. Fax: +91 22 2570.

Notes

The authors declare no competing financial interest.

■ ACKNOWLEDGMENTS

This research is supported by the Australian Research Council (DP0877999) to P.K. and A.D. and a SERC DST grant to A.D. Support from a FIST grant to the Department of Chemistry, IIT Bombay, is gratefully acknowledged. We gratefully acknowledge the Région Haute Normandie for financial support to P.A.P. and A.B. and the Australian Research Council for support of P.K. and S.C. We thank the Ministère des Affaires Etrangères (France) and the Department of Innovation, Industry, Science and Research (Australia) for FAST grants (P.K. and X.F.).

■ REFERENCES

(1) Bell, P. J. L.; Karuso, P. Epicocconone, a Novel Fluorescent Compound from the Fungus *Epicoccum nigrum*. *J. Am. Chem. Soc.* **2003**, *125*, 9304−9305.

(2) Choi, H.-Y.; Veal, D. A.; Karuso, P. Epicocconone, a New Cell-Permeable Long Stokes' Shift Fluorescent Stain for Live Cell Imaging and Multiplexing. *J. Fluoresc.* **2006**, *16*, 475−482.

(3) Chignell, C. F.; Bilski, P.; Reszka, K. J.; Motten, A. G.; Sik, R. H.; Dahl, T. A. Spectral and Photochemical Properties of Curcumin. *Photochem. Photobiol.* **1994**, *59*, 295−302.

(4) Dahl, T. A.; Bilski, P.; Reszka, K. J.; Chignell, C. F. Photocytotoxicity of Curcumin. *Photochem. Photobiol.* **1994**, *59*, 290−294.

(5) Priyadarsini, K. I. Photophysics, Photochemistry and Photobiology of Curcumin: Studies from Organic Solutions, Bio-Mimetics and Living Cells. *J. Photochem. Photobiol., C* **2009**, *10*, 81−95.

(6) Adhikary, R.; Mukherjee, P.; Kee, T. W.; Petrich, J, W. Excited-State Intramolecular Hydrogen Atom Transfer and Solvation Dynamics of the Medicinal Pigment Curcumin. *J. Phys. Chem. B* **2009**, *113*, 5255−5261.

(7) Mackintosh, J. A.; Choi, H. Y.; Bae, S. H.; Veal, D. A.; Bell, P. J.; Ferrari, B. C.; Van Dyk, D. D.; Verrills, N. M.; Paik, Y. K.; Karuso, P. A Fluorescent Natural Product for Ultra Sensitive Detection of Proteins in One-Dimensional and Two-Dimensional Gel Electrophoresis. *Proteomics* **2003**, *3*, 2273−2288.

(8) Ball, M. S.; Karuso, P. Mass Spectral Compatibility of Four Proteomics Stains. *J. Proteome Res.* **2007**, *6*, 4313−4320.

(9) Coghlan, D. R.; Mackintosh, J. A.; Karuso, P. Mechanism of Reversible Fluorescent Staining of Protein with Epicocconone. *Org. Lett.* **2005**, *7*, 2401−2404.

(10) Karuso, P.; Crawford, A. S.; Veal, D. A.; Scott, G. B. I.; Choi, Y.-H. Real-Time Fluorescence Monitoring of Proteolysis. *J. Proteome Res.* **2008**, *7*, 361−366.

(11) Cleemann, F.; Karuso, P. A Fluorescence Anisotropy Assay for the Traceless Kinetic Analysis of Protein Digestion. *Anal. Chem.* **2008**, *80*, 4170−4174.

(12) Panda, D.; Khatua, S.; Datta, A. Enhanced Fluorescence of Epicocconone in Surfactant Assemblies as Consequence of Depth-Dependent Microviscosity. *J. Phys. Chem. B* **2007**, *111*, 1648−1656.

(13) Burai, T. N.; Panda, D.; Datta, A. Fluorescence Enhancement of Epicocconone in Its Complex with Cyclodextrins. *Chem. Phys. Lett.* **2008**, *455*, 42−46.

(14) Chatterjee, S.; Burai, T. N.; Karuso, P.; Datta, A. Ultrafast Dynamics of Epicocconone, A Second Generation Fluorescent Protein Stain. *J. Phys. Chem. A* **2011**, *115*, 10154−10158.

(15) Boulangé, A.; Peixoto, P. A.; Franck, X. Diastereoselective IBX Oxidative Dearomatization of Phenols by Remote Induction: Towards the Epicocconone Core Framework. *Chem.—Eur. J.* **2011**, *17*, 10241−10245.

(16) Stewart, W. W. Synthesis of 3, 6-disulfonated 4-amino-napthalimides. *J. Am. Chem. Soc.* **1981**, *103*, 7615−7620.

(17) Fischer, M.; Georges, J. Fluorescence Quantum Yield of Rhodamine 6G in Ethanol as a Function of Concentration Using Thermal Lens Spectrometry. *Chem. Phys. Lett.* **1996**, *260*, 115−118.

(18) Burai, T. N.; Mukherjee, T. K.; Lahiri, P.; Panda, D.; Datta, A. Early Events Associated with the Excited State Proton Transfer in 2-(2′-pyridyl)benzimidazole. *J. Chem. Phys.* **2009**, *131*, 034504−034508.

(19) TURBOMOLE V6.3 2011, A Development of University of Karlsruhe and Forschungszentrum GmbH.

(20) Grimme, S.; Antony, J.; Ehrlich, S.; Krieg, H. A Consistent and Accurate ab initio Parametrization of Density Functional Dispersion Correction (DFT-D) for the 94 Elements H-Pu. *J. Chem. Phys.* **2010**, *132*, 154104−154119.

(21) Becke, A. D. Density-Functional Exchange-Energy Approximation with Correct Asymptotic Behavior. *Phys. Rev. A* **1988**, *38*, 3098−3100.

(22) Weigend, F.; Häser, M.; Patzelt, H.; Ahlrichs, R. RI-MP2: Optimized Auxiliary Basis Sets and Demonstration of Efficiency. *Chem. Phys. Lett.* **1998**, *294*, 143−152.

(23) Klamt, A.; Schürmann, G. COSMO: A New Approach to Dielectric Screening in Solvents with Explicit Expressions for the Screening Energy and Its Gradient. *J. Chem. Soc., Perkin Trans.2* **1993**, *5*, 799−805.

(24) Schäfer, A.; Huber, C.; Ahlrichs, R. Fully Optimized Contracted Gaussian Basis Sets of Triple Zeta Valence Quality for Atoms Li to Kr. *J. Chem. Phys.* **1994**, *100*, 5829−5835.

(25) Ma, M.; Johnson, K. E. Carbocation Formation by Selected Hydrocarbons in trimethylsulfonium bromide-$AlCl_3$/$AlBr_3$-HBr Ambient Temperature Molten Salts. *J. Am. Chem. Soc.* **1995**, *117*, 1508−1513.

(26) van Walree, C. A.; Roest, M. R.; Schuddeboom, W.; Jenneskens, L. W.; Verhoeven, J. W.; Warman, J. M.; Kooijman, H.; Spek, A. L. Comparison between $SiMe_2$ and CMe_2 Spacers as σ-Bridges for Ohotoinduced Charge Transfer. *J. Am. Chem. Soc.* **1996**, *118*, 8395−8407.

(27) Moss, D. B.; Parmenter, C. S. A Time-Resolved Fluorescence Observation of Intramolecular Vibronic Redistribution within the Channel Three Region of S1 Benzene. *J. Phys. Chem.* **1986**, *90*, 1011−1014.

(28) Syzgantseva, O. A.; Tognetti, V.; Joubert, L.; Boulangé, A.; Peixoto, P. A.; Leleu, A.; Franck, X. Electronic Excitations of Epicocconone Analogues: TDDFT Methodological Assessment Guided by Experiment. *J. Phys. Chem. A* **2012**, *116*, 8634−8643.

(29) Panda, D.; Datta, A. The Role of the Ring Nitrogen and the Amino Group in the Solvent Dependence of The Excited-State Dynamics of 3-aminoquinoline. *J. Chem. Phys.* **2006**, *125*, 054513−054519.